Anal. Bioanal. Electrochem., Vol. 10, No. 4, 2018, 465-477

Analytical & Bioanalytical Electrochemistry

Full Paper

A High-Performance Electrochemical Sensor based on $FeTiO_3$ Synthesis Coated on Conductive Substrates

Dwiprayogo Wibowo[1], Maulidiyah[1], Ruslan[2], Thamrin Azis[1] and Muhammad Nurdin[1,*]

[1]*Department of Chemistry, Faculty of Mathematics and Natural Sciences, Universitas Halu Oleo, Kendari 93232 – Southeast Sulawesi, Indonesia*
[2]*Department of Chemistry, Faculty of Mathematics and Natural Sciences, Universitas Tadulako, Palu 94118 – Central Sulawesi, Indonesia*

*Corresponding Author, Tel.: +6281316551674; Fax: +624013190006
E-Mail: mnurdin06@yahoo.com

Received: 5 February 2018 / Received in revised form: 29 March 2018 / Accepted: 5 April 2018 / Published online: 30 April 2018

Abstract- Conductor substrate-coating ilmenite ($FeTiO_3$) electrodes developed for electrochemical sensors was investigated to high the photocurrent response, which influenced by transfer of electrons for photoelectrocatalytic processes. A highly ordered electrochemical process to obtain the electron response was employed as modeling reduction-oxidation (redox) reactions on working electrodes. This study utilized conductor substrates, i.e., indium tin oxide (ITO), titanium (Ti) plate, and TiO_2/Ti then coated with $FeTiO_3$ sol-gel. The results investigated the resistivity determined in ITO, Ti plate, TiO_2/Ti, $FeTiO_3$/ITO, $FeTiO_3$/Ti, and $FeTiO_3$.TiO_2/Ti electrodes were 21.30 Ω, 0.37 Ω, 5.17 Ω, 117.04 Ω, 31.07 Ω, and 51.24 Ω, respectively. The Ti plate was a better conductor substrate than ITO was indicated by the highest performance with linear sweep voltammetry (LSV) and cyclic voltammetry (CV) methods. The $FeTiO_3$.TiO_2/Ti electrode performance had the highest activity compared with TiO_2/Ti electrode as shown by photocurrent values of 1200 µA and 600 µA, respectively. This phenomenon indicates the photocurrent response of $FeTiO_3$.TiO_2/Ti possesses voltammogram stability for modeling the redox reactions. More importantly, this study to approach of chemical oxygen demand (COD) determination using $FeTiO_3$ synthesized as modeling natural $FeTiO_3$ extracted from mineral sands.

Keywords- $FeTiO_3$, synthesis, sol-gel, electrochemical, sensor

1. INTRODUCTION

Titanium metal can be found in nature and associated with iron (Fe) metal, is known as ilmenite ore ($FeTiO_3$) [1-3]. It is contained in igneous and metamorphic rocks as $FeTiO_3$, TiO_2 (rutile), and titanomagnetite (Fe_2TiO_3-Fe_3O_4) [4,5]. Additionally, within the structure of natural $FeTiO_3$, there still exists other elements, such as Fe_2O_3, MnO, MgO, Al_2O_3 ($(Fe,Mn,Mg)_x(Fe,Al)_yTi_zO_{(x+1,5y+2z)}$ [6]. It has an opaque color, being black to brownish red, with a little sparkle can be categorized as Fe_2O_3-$FeTiO_3$-Fe_3O_4 groups classified as oxides and hydroxides [7]. The utilization of TiO2 material from FeTiO3 mineral has been applied in the manufacture of industrial paints, varnishes, paper, printer ink, coating floors, ceramic, food, and pharmaceuticals [4]. It has been extracted in many countries such as Australia, America, China, Egypt, and Venezuela [8]. $FeTiO_3$ classified as a semiconductor type that containing the titanium-iron oxide mineral. Andreozzi et al. reported that $FeTiO_3$ in nature possesses electrical properties and characteristics vary depending on the composition of atoms distributed in $FeTiO_3$ [9].

$FeTiO_3$ can be obtained naturally from mineral sand extraction and can be formed via a synthesis pathway, specifically the sol-gel method [10,11]. Based on the extraction method, it is difficult to obtain high purity yields based on being highly soluble in acid solutions, whereas the synthesis pathway can be obtained by using Fe^{3+} ions, such as $Fe(NO_3)_3.9H_2O$ [10]. According to Raghavender et al. the synthesis of nano-$FeTiO_3$ using Fe^{3+} ions is better than Fe^{2+} ions because of Fe^{2+} ions are not stable [10]. This condition occurs the distortion mechanism in $FeTiO_3$ structures, so it still requires the stoichiometric ratio and particular physical properties to be analyzed before the characterization process.

The synthesis of nano-$FeTiO_3$ can be formed by solid-state reactions between a mixture of carbon, ilmenite, and argon plasma under high pressure and temperature (1200 °C), but this is not easy because the reaction between the Fe ions and Ti ions takes place spontaneously, creating an unstable $FeTiO_3$ structure [4]. Another advantage to the synthesis of $FeTiO_3$ using the sol-gel method that it is suitable for the coating process, has high stability, and necessitates just low temperatures [12]. It was carried out by substituting the Fe^{3+} ions in Ti^{4+} ions because of the Fe3+ atomic radius ions is smaller (Fe 0.64 Å; 0.68 Å Ti) [13,14].

Many researchers have synthesized nano-$FeTiO_3$ to examine the formation of nanocrystals [15] as well as photocatalytic [16], electrical [17,18], antimicrobial [19], and adsorption [20] because it was considered a renewable material for developing TiO_2 under visible light [21]. Gracia-Munoz et al. reported that a potentially advanced oxidation process causes TiO_2 photocatalysis when the excitation of electron/hole yields the redox reaction mechanism [16]. Photocatalyst technology with a semiconductor is one way to prevent liquid waste problems [22,23]. One benefit of this technology can be degrading organic pollutants into harmless compounds, such as water and CO_2, using redox reactions [24-26]. This process

can be determined by the oxygen demand required to oxidize organic substances contained in organic waste as a parameter of COD [27-30].

Application of $FeTiO_3$ for electrochemical sensors requires variation of conductor substrates based on photogeneration that occurs from the electron transfer that is less stable, consequently the detection of redox is not optimal [31]. It was considered that the electrodes have a resistivity effect in room temperature conditions, so the determination of photocurrent (I) and potential (V) were not accurate [32]. In this study, the photoelectrochemical response from $FeTiO_3$ electrodes synthesized by the sol-gel method was investigated, then coated on ITO, Ti plate, and TiO_2/Ti to demonstrate photocurrent response profile as the working electrodes to detect the organic pollutant as COD.

2. EXPERIMENTAL METHODS

2.1. Preparation of Conducting Substrates

ITO substrate was cleaned by using ethanol solution and scrubbing by cotton on the surface then drying in room temperature. While, the Ti plate was prepared by sanded with 1200 CC fine sandpaper, then washed with the detergent, water, and distilled water. Subsquently, it was immersed (etching) using a mixed solution of HF, HNO_3, and distilled water (1:3:6) for two minutes. The preparation of TiO_2/Ti by anodization method was carried out for 4 h using electrolyte solution in the 0.27 M NH_4F, distilled water, 98% gycerol. The final stage was calcination for 1.5 h with temperature 450 °C to evaporate the electrolyte solution and to obtain crystals of TiO_2 anatase.

2.2. Preparation of $FeTiO_3$ nanoparticles

$FeTiO_3$ nanoparticles were synthesized by using the sol-gel method, where the $Fe(NO_3)_3.9H_2O$ reacted with Titanium tetraisopropoxide (TTIP), acetylacetone, citric acid, deionized water, and ethanol were refluxed and heated to 50 °C for 3 h. Subsequently, the $FeTiO_3$ sol was evaporated during 48 h at room temperature and calcinated on 80 °C to obtain the $FeTiO_3$ sol-gel. Immobilization on ITO, Ti plate, and TiO_2/Ti electrodes by using solvent casting; the electrodes have immersed in $FeTiO_3$ sol-gel then evaporated during 48 h. Finally, the electrodes were calcinated at 450 °C.

2.3. Characterizations

Electrochemical test of ITO, Ti plate, TiO_2/Ti, $FeTiO_3$/ITO, $FeTiO_3$/Ti and $FeTiO_3.TiO_2$/Ti electrodes by using potentiostat DY2100B (Digi-Ivy) with linear sweep voltammetry (LSV), cyclic voltammetry (CV), and multi-pulse amperometry (MPA) programs. The conductivity of electrodes was determined by using multimeter test.

3. RESULTS AND DISCUSSION

3.1. Resistivity determines on working electrodes

The resistivity testing of the electrodes was determined with a digital multimeter which is contacted on the surface. The electron transfer data has measured before and after coating with $FeTiO_3$ sol-gel.

Fig. 1 showed the comparison of resistivity versus condutivity on each substrates which is determination by equations:

$$\rho = R.l \tag{1}$$

$$\sigma = \frac{1}{\rho} \tag{2}$$

Where: ρ = resistivity (Ω.cm), σ = conductivity ($\Omega^{-1}.cm^{-1}$), R = resistance (Ω), *l* = substrates length (cm).

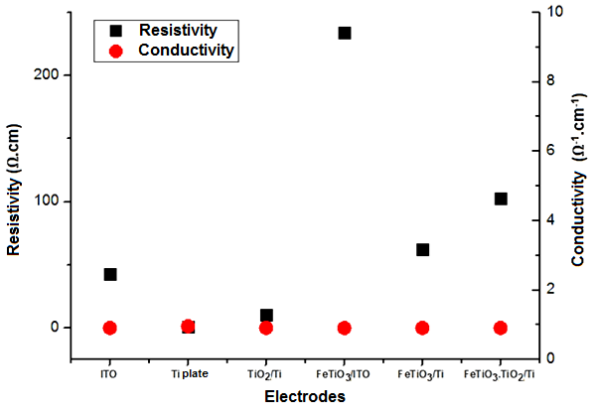

Fig. 1. Comparison data of resistivity and conductivity of electrodes

Table 1. Determination of resistivity and conductivity from working electrodes

l(cm)	Electrodes	Resistance (Ω)			Average (Ω)±STD	Resistifity ρ (Ω.cm)	Conductivity σ ($\Omega^{-1}.cm^{-1}$)
		1	2	3			
	ITO	22.50	20.60	20.80	21.30±1.05	42.60	0.024
	Ti plate	0.40	0.30	0.40	0.37±0.05	0.74	1.352
2	TiO_2/Ti	5.80	3.80	5.90	5.17±1.18	10.34	0.097
	$FeTiO_3$/ITO	115.50	116.60	119.0	117.04±1.79	234.07	0.004
	$FeTiO_3$/Ti	29.67	32.05	31.49	31.07±1.25	62.14	0.016
	$FeTiO_3.TiO_2$/Ti	51.70	53.40	48.60	51.24±2.44	102.47	0.009

Fig. 1 shows the increase of resistivity following coating by $FeTiO_3$ sol-gel. The immobilization on the ITO electrode exhibited the highest of resistivity when compared with TiO_2/Ti and Ti plate, but the conductivity test after coating showed it was same with all having the same average values. According to Chan et al. the increase in resistivity from ITO substrate caused a thin film effect from indium, tin, and oxygen that is categorized as a semiconductor with a band gap of 3.5-4.3 eV [33].

Table 1 showed the resistivity results on the electrodes were determined in repetitions of three and calculated with average values. Based on the data, the resistivity average value for ITO, Ti plate, TiO_2/Ti, $FeTiO_3$/ITO, $FeTiO_3$/Ti, and $FeTiO_3$.TiO_2/Ti electrodes were 21.30 Ω, 0.37 Ω, 5.17 Ω, 117.04 Ω, 31.07 Ω, and 51.24 Ω, respectively. The resistivity of ITO had a higher value because it was formed by indium, tin, and oxides, then coated on glass. It influenced the conductivity of electricity, followed by the addition of $FeTiO_3$ sol-gel, so the resistivity value was elevated on the $FeTiO_3$/ITO electrode. Meanwhile, the immobilization on the Ti plate and TiO_2/Ti had been low resistivity because of the electrons were free to move between the nuclei, then involve the binding interactions with charged ions. $FeTiO_3$ was categorized as a semiconductor based on the increase in the electrode resistivity [9,10].

3.2. Wavelength Absorption Spectra on Substrate Conductor

Fig. 2 shows the absorbance range of conductive substrates using a UV-Vis spectrophotometer. The absorption of ITO did not contribute energy absorption, because of the energy was transmitted and reflected [34]. Ti plate explained a weak absorption spectrum possibility the reaction of O_2 (air) to form an oxide thin film on the Ti surface. Subsequently, the TiO_2/Ti was active under UV light that proved the wavelength scanning absorption in 388 nm (3.2 eV) UV was better than Visible regions [35].

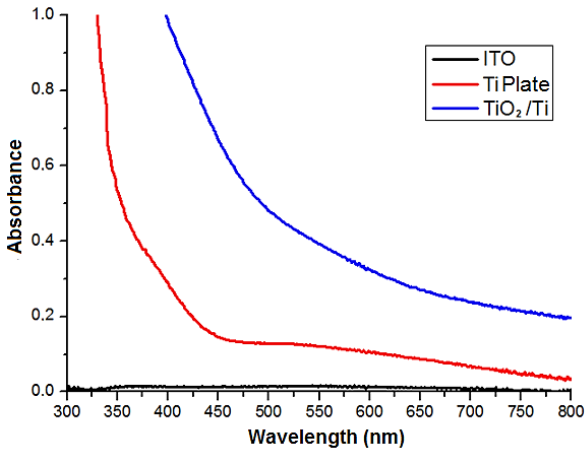

Fig. 2. The absorption of substrates conductor

3.3. Electrochemical Test

3.3.1. Linear sweep voltammetry (LSV)

Fig. 3 shows the determination of photocurrent by 0.1 M $NaNO_3$ as an electrolyte that illustrating the oxidation process occurs via photocurrent using the photoelectrocatalytic system [36].

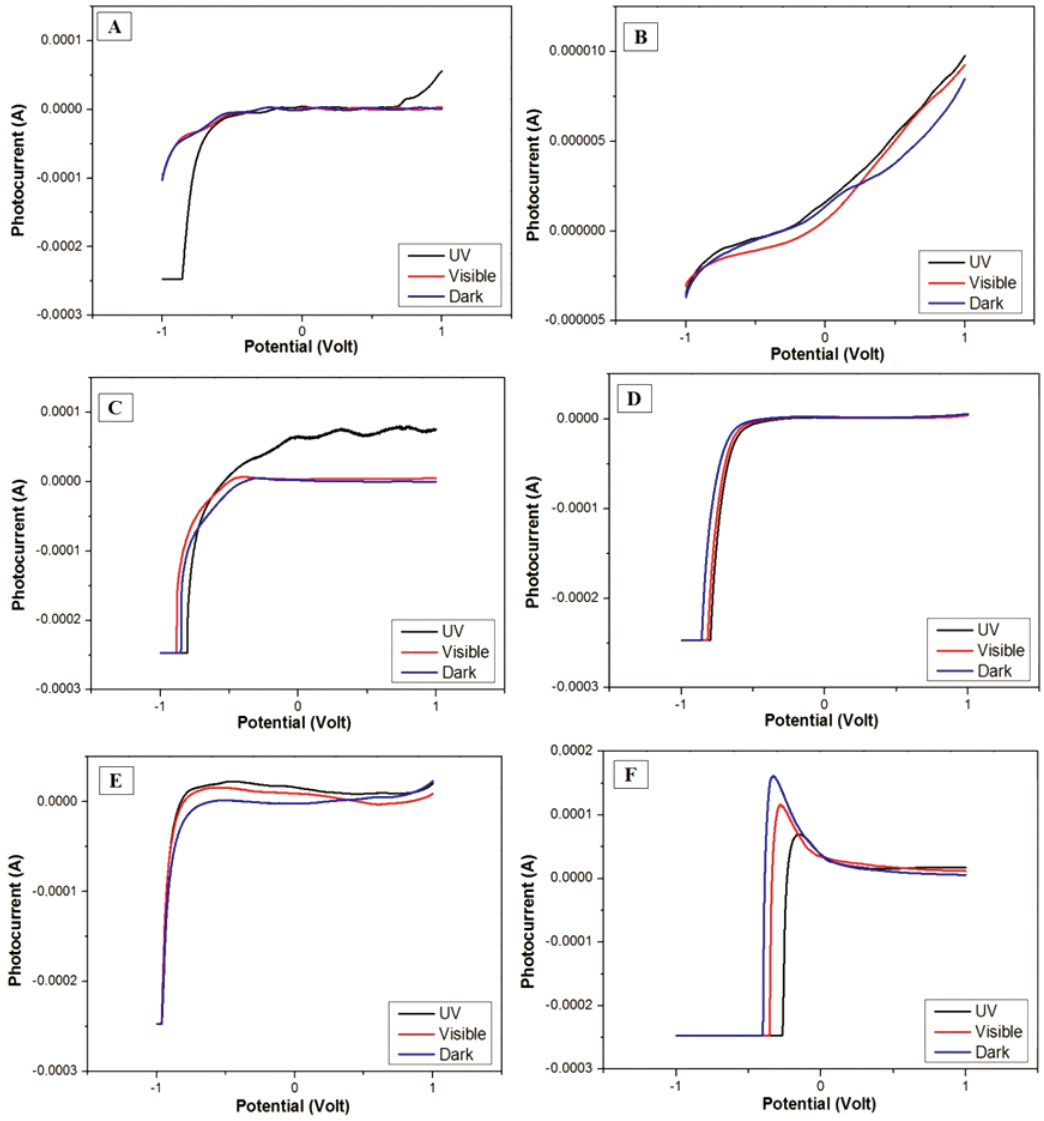

Fig. 3. LSV electrochemical profile on electrodes: (A) ITO, (B) Ti plate, (C) TiO_2/Ti, (D) $FeTiO_3$/ITO, (E) $FeTiO_3$/Ti, and (F) $FeTiO_3$.TiO_2/Ti

The variation of UV and visible lights to obtain the photocurrent response were induced by a photon. Fig. 3A shows the performance of ITO electrode does not have a higher peak, suggesting it does not follow an oxidation process. Fig. 3B indicated electrons moving simultaneously in Ti plate, because there is no a semiconductor layer formed on the surface, so there is an increase of electron transfer, exhibiting the flowing current detected by the

potentiostat. Fig. 3C shows the highest peak with irradiation by UV light on TiO_2/Ti. According to Maulidiyah et al TiO_2/Ti has high activity in terms of transferring electrons when irradiation of UV light because it has a band gap of 3.2 eV, needing higher energy for electron excitation [37]. Fig. 3D showed the lower $FeTiO_3$/ITO performance compared to Fig. 3E and 3F, caused a higher photocurrent, indicating of oxidation process and potential activity in visible light [10,38]. Based on Fig. 3F, there is much oxidation compare with $FeTiO_3$/Ti (Fig. 3E) because the movement of electrons from $FeTiO_3$ then transferred to TiO_2 as a semiconductor for electron stability and neutralization.

3.3.2. Cyclic Voltammetry (CV)

Fig. 4 shows the results of CV performed to characterize the working electrodes in contact with the electrolyte [39]. It was polarized in a redox direction up to -2 V and back up to 0.5 V with Ag/AgCl 0.1 M $NaNO_3$ as the electrolyte.

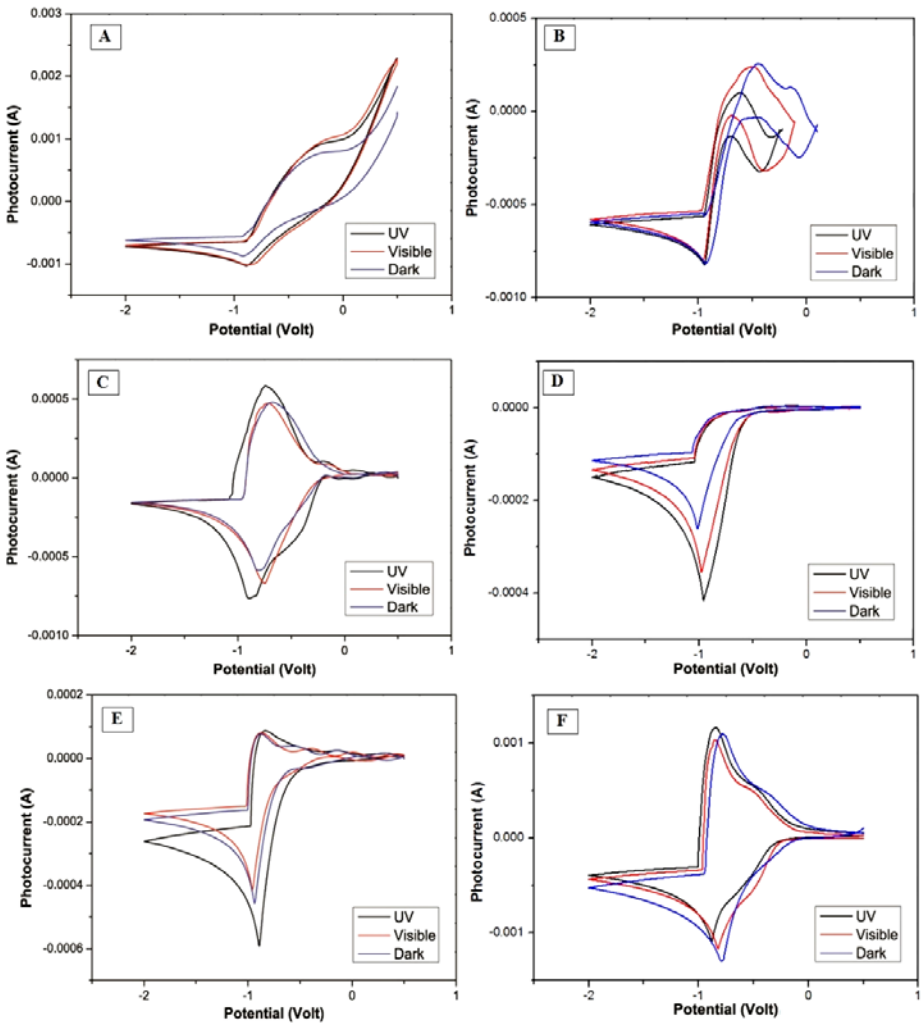

Fig. 4. CV electrochemical profile on electrodes: (A) ITO, (B) Ti plate, (C) TiO_2/Ti, (D) $FeTiO_3$/ITO, (E) $FeTiO_3$/Ti, and (F) $FeTiO_3$.TiO_2/Ti

Dechakiatkrai et al. reported by using $NaNO_3$ electrolyte, the highest photocurrent can be applied in a TiO_2 semiconductor [40]. Fig. 4A, 4B, and 4D illustrate very low capacitive photocurrent, but in the cathodic range, there is much rich electrochemical activity, whereas in Fig. 4C, 4E, and 4F, the higher capacitive photocurrent in anodic and cathodic potentials is portrayed, and it was considered that the performance of electron transfer using Ti plate as substrate was better than ITO.

$FeTiO_3.TiO_2$/Ti and TiO_2/Ti had the highest stability within redox reactions as demonstrated with the high peak corresponding to photocurrent values of 1200 µA and 600 µA, respectively. Based on Weber et al. the Fe ions adhered to the oxidation mechanism in the $NaNO_3$ electrolyte, whereas the Fe^{2+} ions were chemically oxidized and a thicker oxide layer on the surface of working electrodes was formed [41]. In the mechanism shown:

$$Fe \rightarrow Fe^{2+} + 2e^{-} \quad (3)$$

If the electrode surface is covered with an oxide layer, passive dissolution takes place according to,

$$Fe \rightarrow Fe^{3+} + e^{3-} \quad (4)$$

is also possible. In the presence of oxygen, an oxidation of Fe^{2+} to Fe^{3+} is also possible:

$$Fe^{2+} \rightarrow Fe^{3+} + e^{-} \quad (5)$$

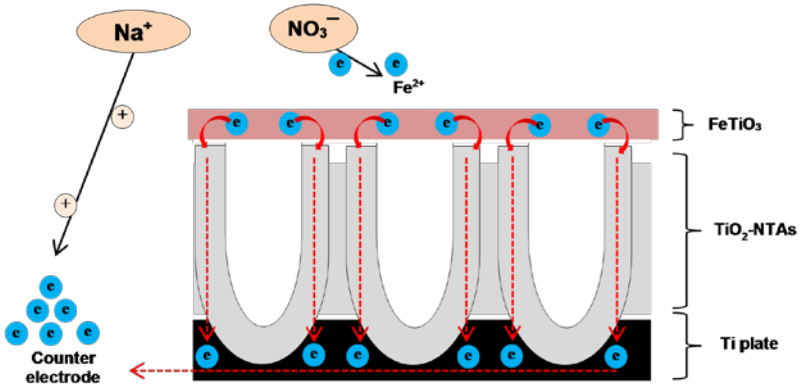

Fig. 5. Purpose mechanism on $FeTiO_3.TiO_2$/Ti electrode surface by $NaNO_3$ electrolyte solution

3.3.3. Multi Pulse Amperometry (MPA)

Fig. 6 shows the amperometry results of $FeTiO_3.TiO_2$/Ti electrode. The photoelectrochemical process can be determined by a potentiostat which is induced with UV irradiation where the electron transfer is reflected by photocurrent values to inform oxidation. This determination based on a photoelectrochemical process whereby the combination of photocatalytic and electrocatalytic processes induced a bias potential of 0.5 V to separate

electrons by photocatalytic (valence band to conduction band), at which point the electrons were carried to a Pt electrode as a reference electrode. This phenomenon applied to all organic compound degradation processes in a photoelectrocatalysis system.

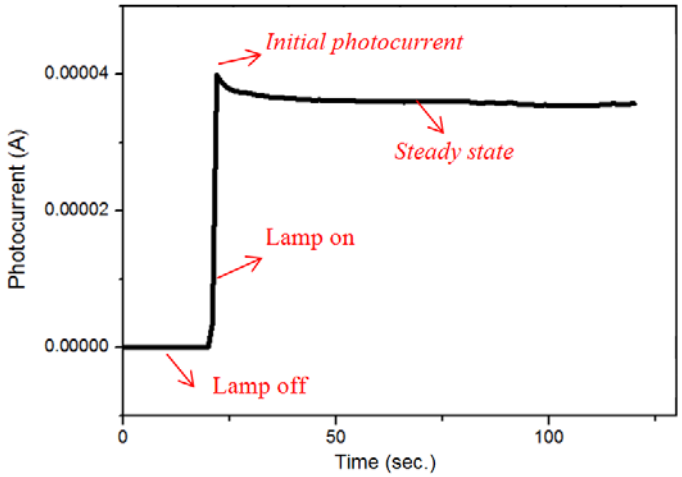

Fig. 6. Amperometric electrochemical profile as determining the COD value

Fig. 7A explained the photocurrent profile activity for $FeTiO_3.TiO_2$/Ti, when UV irradiation brought about photocurrent transition. Xu et al. described a high-quality optical response on the electrode [42], where the photocurrent value was 338 µA. Meanwhile, the dark state of photocurrent density could be ignored by assuming the electrons were in their ground state [39]. Fig. 7B supports the variation induced with UV and visible lights, specifically showing the photocurrent response as electron transfer diminishes with visible light. This indicates that the photocurrent response was not optimal, but could still elicit electron separation.

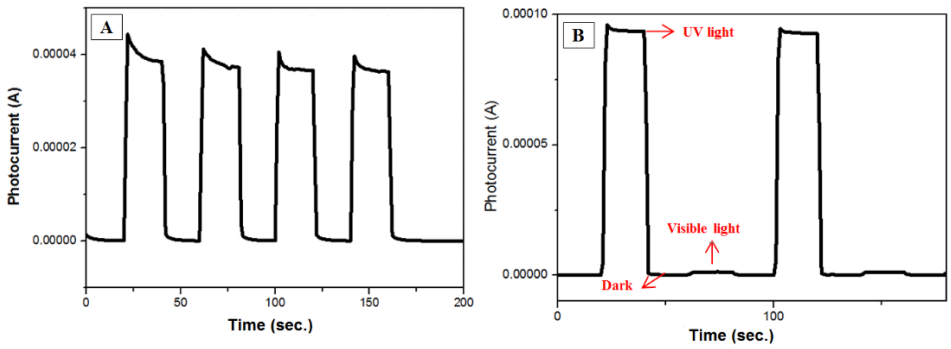

Fig. 7. Photoelectrochemical profile using $FeTiO_3.TiO_2$/Ti

Fig. 8 is a schematic illustration of the reaction mechanism on the $FeTiO_3.TiO_2$/Ti electrode by irradiating UV and visible lights. The photocurrent response total transfer of electrons with UV light induction yields a greater value, while visible light is as low

photocurrent. This can be determined using a potentiostat based on its capability of possible electron excitation with UV and visible irradiation. The recombination of electrons can take place with irradiation by visible light based on the band gap state near the valence band.

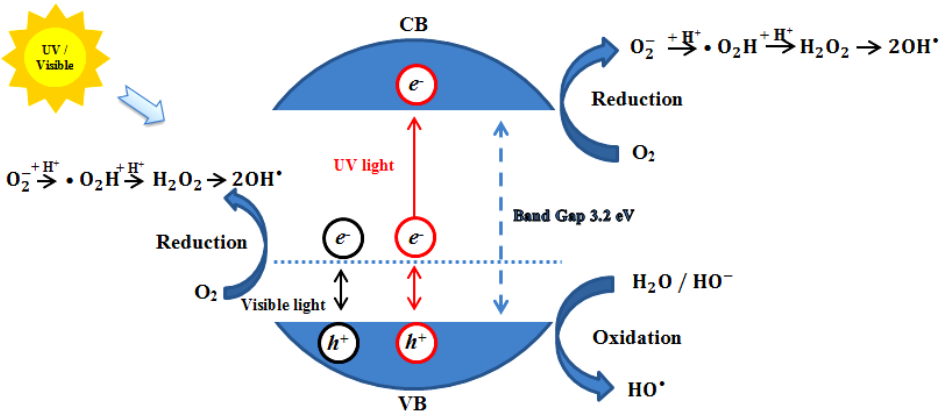

Fig. 8. Purpose of schematic reaction on $FeTiO_3$.TiO_2/Ti by photoelectrochemical

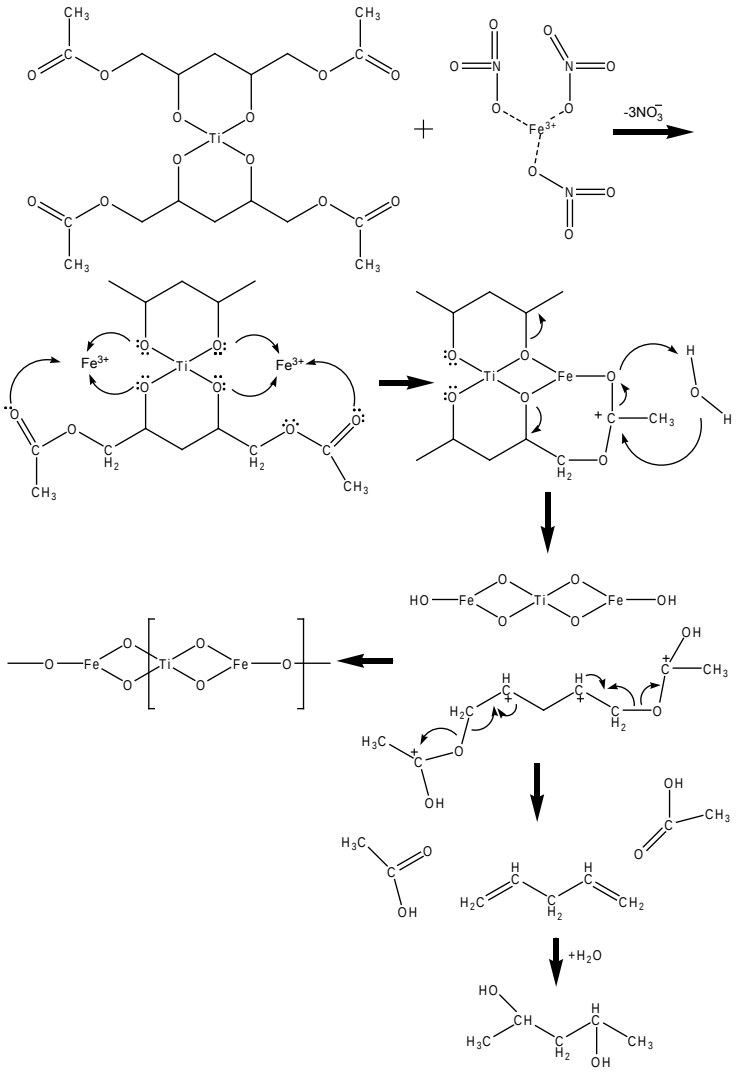

Fig. 9. Purpose of $FeTiO_3$ synthesis mechanism by sol-gel method

3.4. $FeTiO_3$ synthesis pathway using sol-gel method

Fig. 9 described the proposed mechanism of $FeTiO_3$ synthesis pathway using the sol-gel method. Generally, the TTIP as the titanium source was modified with acetylacetonate, H_2O, and acetic acid in ethanol solutions [35]. The electrons are free from O atoms and attack the Fe^{3+} ions to form ....-TiO_2-Fe-O-C^+CH_3-O-... It was thought that the distortion affected the crystal form. Subsequently, the C^+ was separated from the bond. Finally, the ...-O-Fe-TiO_2-Fe-O- ...bonds were crystallized to form in organic solvents, like acetic acid and alcohol derivatives. This change of color to orange-brown indicated there was no agglomeration.

4. CONCLUSION

Based on the investigation, the Ti plate was better than ITO as conductor substrate after coating $FeTiO_3$. determination of resistivity on ITO, Ti plate, TiO_2/Ti, $FeTiO_3$/ITO, $FeTiO_3$/Ti, and $FeTiO_3$.TiO_2/Ti electrodes were 21.30 Ω, 0.37 Ω, 5.17 Ω, 117.04 Ω, 31.07 Ω, and 51.24 Ω, respectively. The $FeTiO_3$.TiO_2/Ti electrode was highest activity compared with TiO_2/Ti electrode by photocurrent values of 1200 µA and 600 µA. The photoelectrochemical process using $FeTiO_3$.TiO_2/Ti was responsive to UV and visible lights. In general, this study an approach for determining COD employing $FeTiO_3$ synthesized by modeling natural $FeTiO_3$ extracted from mineral sands.

Acknowledgements

The authors would like to express their appreciation for the financial support of the Ditlitabmas-Dikti Ministry of Research, Technology and Higher Education, the Republic of Indonesia and Pusat Penyelidikan-Institute of Microengineering and Nanoelectronics – Universiti Kebangsaan Malaysia for valuable contribution in obtaining instrument measurements.

REFERENCES

[1] M. G. Shahhien, M. M. H. Khedr, A. E. Maurice, A. A. Farghali, and R. A. M. Ali, Beni-Suep Univeristy J. Basic & Appl. Sci. 4 (2015) 207.

[2] M. Nurdin, Maulidiyah, A. H. Watoni, N. Abdillah, and D. Wibowo, Int. J. Chem. Tech. Res. 9 (2016) 483.

[3] M. Nurdin, A. Zaeni, Maulidiyah, M. Natsir, A. Bampe, and D. Wibowo, Orient. J. Chem. 32 (2016) 2113.

[4] S. Samal, and D. W. Park, Chem. Eng. Res. Design 90 (2012) 548.

[5] S. Samal, B. K. Mohapatra, P. S. Mukherjee, and S. K. Chatterjee, J. Alloys Compounds 474 (2009) 484.

[6] C. S. Kucukkaragoz, and R. H. Eric, Mineral Eng. 19 (2006) 334.
[7] V. S. Gireesh, V. P. Vinod, S. K. Nair, and G. Ninan, Int. J. Mineral Process. 134 (2015) 36.
[8] R. Vasquez, and A. Molina, Metal 5 (2008) 13.
[9] G. B. Andreozzi, F. Cellucci, and D. Gozzi, J. Mater. Chem. 6 (1996) 987.
[10] A. T. Raghavender, N. H. Hong, K. J. Lee, M. H. Jung, Z. Skoko, M. Vasilevskiy, M.F. Cerqueira, and A. P. Samantilleke, J. Magnetism Magnetic Mater. 331(2013) 129.
[11] A. B. Gambhire, M. K. Lande, S. B. Rathod, B. R. Arbad, K. N. Vidhate, R. S. Gholap, and K. R. Patil, Arabian J. Chem., 9 (2016) S429.
[12] M. Zarazua-Morin, L. M. Torres-Martinez, E. Moctezuma, I. Juarez-Ramirez, and B. B. Zermeno, Res. Chem. Intermediates 42 (2015) 1029.
[13] N.C. Wilson, S.P. Russo, J. Muscat, N.M. Harrison, Phys. Rev. B 72 (2005) 1.
[14] J. Yu, Z. Wu, C. Gong, W. Xiao, L. Sun, and C. Lin, Nanomaterials 6 (2016) 1.
[15] J. Yu, Y. Chen, and A. M. Glushenkov, Crystal Growth Design 9 (2009) 1240.
[16] P. Gracia-Munoz, G. Pliego, J. A. Zazo, A. Bahamonde, and J. A. Casas, J. Environ. Chem. Eng. 4 (2016) 542.
[17] A. Mehdilo, M. Irannajad, and B. Rezai, Coll. Surfaces A 428 (2013) 111.
[18] A. Mehdilo, M. Irannajad, and B. Rezai, Mineral Eng. 70 (2015) 64.
[19] D. Sethi, N. Jada, R. Kumar, S. Ramasamy, S. Pandey, T. Das, J. Kalidoss, P.S. Mukherjee, and A. Tiwari, J. Photochem. Photobiol. 140 (2014) 69.
[20] Y. H. Chen, J. Non-Crystalline Solids 357 (2011) 136.
[21] W. Zhang, Z. Zhu, and C. Y. Chen, Hydrometallurgy 108 (2011) 177.
[22] Maulidiyah, H. Ritonga, C. E. Faiqoh, D. Wibowo, and M. Nurdin, Biosci. Biotechnol. Res. Asia 12 (2015) 1985.
[23] Maulidiyah, D. Wibowo, Hikmawati, R. Salamba, and M. Nurdin, Orien. J. Chem. 31 (2015) 2337.
[24] Hikmawati, A. H. Watoni, D. Wibowo, Maulidiyah, and M. Nurdin, IOP Conf. Series: Mater. Sci. Eng. 267 (2017) 012005.
[25] Maulidiyah, H. Ritonga, R. Salamba, D. Wibowo, and M. Nurdin, Int. J. Chem. Tech. Res. 8 (2015) 645.
[26] Z. Arham, M. Nurdin, and B. Buchari, Int. J. Chem. Tech. Res. 9 (2016) 113.
[27] Maulidiyah, M. Nurdin, Erasmus, D. Wibowo, M. Natsir, H. Ritonga, and A. H. Watoni, Int. J. Chem. Tech. Res. 8 (2015) 416.
[28] P. Perreault, and G. S. Patience, Fuel 165 (2016) 166.
[29] Maulidiyah, D.S. Tribawono, D. Wibowo, and M. Nurdin, Anal. Bioanal. Electrochem. 8 (2016) 761.
[30] Z. Zhang, X. Chang, and A. Chen, Sens. Actuators B 223 (2016) 664.

[31] D. Wibowo, Ruslan, Maulidiyah, and M. Nurdin, IOP Conf. Series: Mater. Sci. Eng. 267 (2017) 012007.
[32] D. K. Behara, G. P. Sharma, P. Upadhyay, M. Gyanprakash, R. G. S. Pala, and S. Sivakumar, Chem. Engin. Sci. 154 (2016) 150.
[33] S. H. Chan, M. C. Li, H. S. Wei, S. H. Chen, and C. C. Kuo, J. Nanomater. 2015 (2015) 1.
[34] M. K. M. Ali, K. Ibrahim, O. S. Hamad, M. H. Eisa, M. G. Faraj, and F. Azhari, Romanian J. Phys. 56 (2011) 730.
[35] Maulidiyah, M. Nurdin, E. Widianingsih, T. Azis, and D. Wibowo, ARPN J. Engin. Appl. Sci. 10 (2015) 6250.
[36] M. Nurdin, M. Z. Muzakkar, M. Maulidiyah, M. Nurjannah, and D. Wibowo, J. Mater. Environ. Sci. 7 (2016) 3334.
[37] Maulidiyah, M. Nurdin, D. Wibowo, and A. Sani. Int. J. Pharma. Pharmaceu. Sci. 7 (2015) 141.
[38] Ruslan, M. Mirzan, M. Nurdin, and A. W. Wahab, Int. J. Appl. Chem. 12 (2016) 399.
[39] M. Nischk, P. Mazierski, Z. Wei, K. Siuzdak, N. A. Kouame, E. Kowalska, H. Remita, and A. Zaleska-Medynska, Appl. Surf. Sci. 387 (2016) 89.
[40] C. Dechakiatkrai, J. Chen, C. Lynam, S. Phanichphant, and G. G. Wallace, J. Electrochem. Soc. 154 (2007) A407.
[41] O. Weber, M. Weinmann, H. Natter, and D. Bahre, J. Appl. Electrochem. 45 (2015) 591.
[42] H. M. Xu, H. Wang, J. Shi, Y. Lin, and C. Nan, Nanomaterials 6 (2016) 1.